JMEPEG (2010) 19:1001–1004
DOI: 10.1007/s11665-010-9605-5

1059-9495/$19.00

Effect of Surface Roughness on the Oxidation Behavior of the Ni-Base Superalloy ME3

Jeffrey L. Evans

(Submitted December 3, 2009; in revised form January 4, 2010)

Ni-base superalloys are used in applications, such as jet aircraft engines and power production facilities that require excellent elevated temperature oxidation resistance. This present work evaluated the effect of surface roughness on the oxidation behavior of the Ni-base superalloy ME3. Isothermal oxidation tests were performed in air at different times to investigate the oxide growth kinetics. The surface oxides were also characterized using scanning electron microscopy and x-ray diffraction. The surface roughness was measured using a linear scanning profilometer. The surface roughness measurements were correlated to the oxidation rates and an empirical model is proposed to describe the effect of surface roughness on the oxidation behavior.

Keywords corrosion testing, superalloys, surface engineering

1. Introduction

Ni-base alloys exhibit oxidation resistance by forming a protective, passive oxide layer. These alloys are classified into those that form chromia and those that form alumina protective scales. The alumina forming alloys have higher temperature oxidation resistance. The chromia-based alloys are limited in their high temperature use because the protective oxide decomposes into a volatile CrO_3 above 900-950 °C, leaving the oxide nonprotective (Ref 1). Depending on the alloy, these materials can also form other oxides such as NiO, FeO, and $Ni(FeCr)_2O_4$ (Ref 2).

Oxidation and the subsequent formation of a protective oxide layer are time-dependent processes. During the transient between the early stages of oxidation and passivation, potential damage could occur to the underlying alloy. Also, if a fatigue crack is progressing through a component, then each cycle would require re-passivation. The time period prior to passivation could allow oxygen to penetrate through the surface of the material and cause internal damage. Therefore, it is critical to understand the early stage oxidation kinetics (Ref 3).

The surface roughness has been shown to play a role in the oxidation behavior for a number of materials (Ref 4-7). For an Fe-Cr-Al material, the composition of the oxide scale and the scale thickness differed depending on the starting sample surface finish. This indicated that for this material the surface roughness influenced the composition and growth rate of the nucleating oxide (Ref 5). When pure nickel was exposed to elevated temperature, the growth rate of the NiO was shown to be determined by the starting surface finish of the sample. A faster oxidation rate was seen with greater surface roughness (Ref 6). The surface roughness also was shown to affect the early stages of oxide formation on Fe-Al and Fe-Cr-Al alloys (Ref 7). In that study greater surface roughness was shown to produce iron-rich nodules. The conclusion was that the greater surface roughness provided enhanced cold work which in turn increased the diffusion rate of Fe. This effect was also seen for chromia-forming alloys, where the increased surface roughness enhanced the Cr_2O_3 formation by increasing the diffusion rate of Cr (Ref 7).

Jeffrey L. Evans, Department of Mechanical and Aerospace Engineering, University of Alabama in Huntsville, Huntsville, AL 35603. Contact e-mail: Jeff.Evans@uah.edu.

2. Experimental Procedures

The material used for this study was the Ni-base superalloy ME3, a powder metallurgy processed advanced jet engine disk alloy developed by the NASA Glenn Research Center, General Electric, and Pratt & Whitney. The composition of the material used for these tests is shown in Table 1. The material was machined into samples having dimensions 12.7 mm × 12.7 mm × 2.54 mm.

The surfaces of the samples were prepared using sequentially finer grit SiC paper. Samples were prepared having final finishes of 220, 600, and 1200 grit SiC. The surfaces of the samples were ultrasonically cleaned with a detergent solution and subsequently rinsed with flowing water. The surface roughness was measured using a two-dimensional scanning profilometer. Three scans were conducted on each side of each sample.

The dimensions and the mass of the samples were measured. The mass was measured to the nearest 0.1 mg. The samples were exposed at 704 °C (an expected temperature for this alloy in a turbine disk application) in a Lindberg tube furnace. After each exposure time of 1, 10, 15, 20, and 31 h, the mass of each sample was measured. The short exposure times were chosen to evaluate the surface roughness effects on the early transient oxidation period.

At the end of the 31 h exposure, the oxides were evaluated using a JEOL JSM 7000F scanning electron microscope (SEM), an energy dispersive spectroscopy system (EDS), and a Bruker GADDS X-ray diffractometer (XRD), all of which are located at the Central Analytical Facility at the University of Alabama at Tuscaloosa.

Table 1 Chemical composition of ME3 in weight percent

Alloy	C	Cr	Ni	Co	Mo	W	Nb	Ti	Al	Fe	B	Other
ME3	0.056	12.7	50.760	20.6	3.9	2.0	0.89	3.5	3.2	···	0.033	0.050Zr, 0.001 Mg, 2.3Ta

Table 2 The average RMS surface roughness for each of the three surface finishes

SiC grit	Avg RMS roughness, μm	Standard deviation
220	231.0	171.1
600	159.6	170.7
1200	48.1	45.4

3. Results and Discussion

The average RMS surface roughness for each SiC grit size is shown in Table 2. The average values were calculated from three scans taken on each side of three samples prepared with each of the three finishes. Therefore, each value is the average of 18 individual measurements.

The average RMS roughness is lowest for the finest surface finish (1200 grit SiC) and largest for the coarsest surface finish (220 grit), as would be expected. However, significant variation was observed in the individual measurements, as is seen with the standard deviation values. This indicates that either more scans are needed to get a better average or that more care needs to be taken in the surface preparation to ensure the surface finish is as uniform as possible on each surface. Never-the-less, for the purpose of this comparison study, the average RMS roughness values were used when comparing oxidation behaviors.

The samples were oxidized in a tube furnace, removed, weighed, and placed back in the furnace after each length of exposure. The mass measured after 1 h exposure was substantially less than the initial mass before exposure. The expected result is for the mass to increase with time as oxygen reacts with the metal surface, unless spallation occurs and the oxide scale is not contained. However, for this study the samples were placed in covered crucibles to capture any spalled oxide. The initial and post-exposure mass measurements were conducted on the crucible with the sample inside. Therefore, the results after 1 h indicate some moisture or other contaminants were baked off of the crucible during the exposure at elevated temperature. Given this discrepancy, the subsequent mass gain calculations for 10, 15, 20, and 31 h were made relative to the 1 h mass measurements. The mass gain was calculated using Eq 1.

$$m'' = \frac{\Delta m}{A} = \frac{W_F - W_O}{A}, \qquad \text{(Eq 1)}$$

where W_F is the final mass, W_O is the original mass, and A is the surface area. For this study, the original mass was the mass after 1 h exposure. This is not too unreasonable given the very slow oxidation kinetics at this temperature. The mass gain relative to the 1 h exposure measurements as a function of time is shown in Fig. 1. Each data point is the average of three samples.

In all cases, the mass gain was higher for the roughest surface, the 220 grit surface finish. The 600 grit and the 1200 grit surfaces had very similar mass gain for the 10 and 20 h exposures and differed for the 15 and 30 h exposures with the 600 grit being higher after 15 h and the 1200 grit being slightly higher after 31 h. This may indicate that no mass gain difference exists between 600 and 1200 grit at this temperature and for these times. Also, a concern with this study is that at these relatively short exposure times and relatively low temperatures, the actually mass gain may not be adequately captured with a measurement resolution of 0.1 mg. The mass gain for the 220 grit surface finish, however, is distinctly higher than the other two surface finishes after all times tested. This may suggest the same cold work/surface roughness effect seen in the other studies previously mentioned.

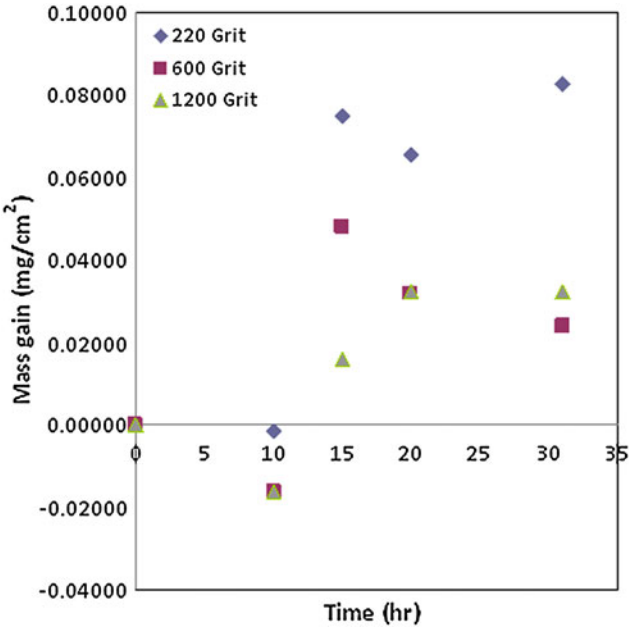

Fig. 1 Mass gain as a function of time at 704 °C

The mass gain as a function of the RMS roughness is presented in Fig. 2. From these results, the linear regression analysis was used to develop an empirical model for the effect of the surface roughness on the mass gain for each time, which is shown in Fig. 2 for the 10, 15, 20, and 31 h exposures. For all exposure times, the slope is positive suggesting an increasing mass gain with increasing initial surface roughness.

After 31 h of elevated temperature exposure, the surface oxides were evaluated using the SEM. Representative images for each of the three surface finishes are shown in Fig. 3. A layer consisting of oxide particles was seen on the surfaces of all the samples. The surfaces had very similar features for all three sample types; however, the oxide particles present on the sample with a 220 grit surface finish seemed to be somewhat larger in size than those present on the 600 and 1200 grit samples. It may be that increased Cr diffusion to the surface due to the larger surface roughness/cold work is more prevalent in the sample prepared to a 220 grit surface finish. This enhanced diffusion could act to nucleate oxide particles faster and therefore create more of them than is seen on the samples with the smoother initial surfaces.

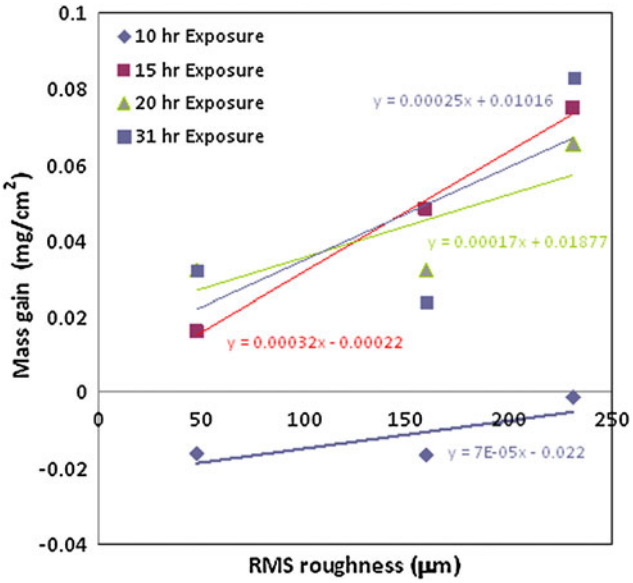

Fig. 2 Mass gain as a function of the RMS roughness

An EDS analysis was conducted to determine the composition of the oxides. For all samples, the percent oxygen was from 16% to 21%, indicating that the surface layer is an oxide. The base ME3 material has ~50% nickel. The percentage nickel observed on these oxidized samples was from 37% to 42%, suggesting the oxide was not nickel but was covering the nickel in the base material. The percentage Cr in the oxide layer was 11–13%, which is similar to that found in the base material, indicating that the oxide layer for all cases was most likely a chromium oxide.

The sample surfaces were also analyzed using x-ray diffraction (XRD). This technique allows the identification of the specific phases present in a material. In this study, XRD was used in an attempt to identify the oxides present. The configuration of the instrument may not have sufficiently allowed the best analysis of the thin oxide scales. The most readily identifiable x-ray peaks obtained were for the base alloy. These peaks dominated the spectra for each sample. However, a very small Cr_2O_3 peak and/or a peak for the spinel oxide $NiCr_2O_4$ were seen on all the oxides. The peaks are very close for both of these oxides and both may be present. A thicker oxide would help in making the identification.

4. Conclusions

The following conclusions were obtained from this study:

1. The initial surface roughness has an effect on the oxidation rate, with the largest surface roughness providing the largest mass gain for 10, 15, 20, and 31 h at 704 °C.
2. The mass gain increased with an increasing initial surface roughness at all times investigated.
3. A Cr-rich oxide was present on the surfaces of all the samples.
4. Larger oxide particles were observed on the sample with the 220 grit surface finish as compared to the 600 and 1200 grit samples.

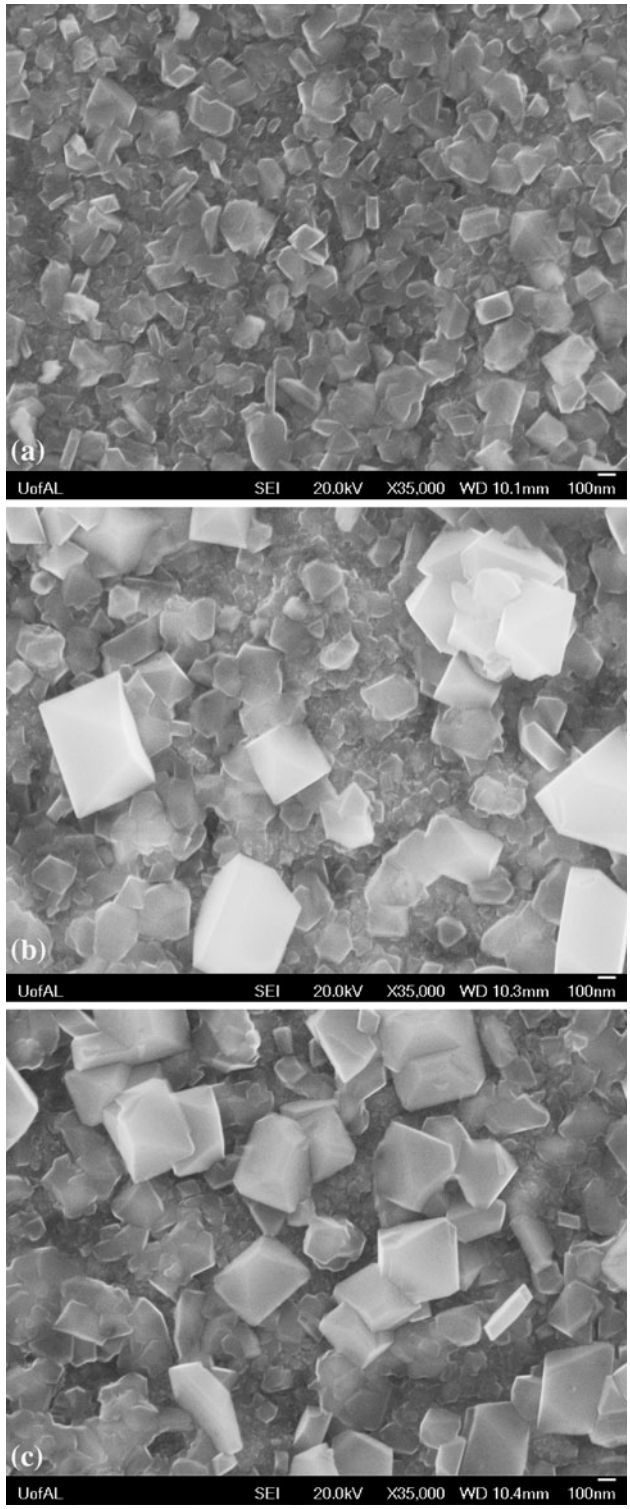

Fig. 3 SEM images of the (a) 220, (b) 600, and (c) 1200 grit specimens after 31 h at 704 °C

Acknowledgments

The author gratefully acknowledges the University of Alabama in Huntsville Mini-Grant Program for funding. The material was supplied by the NASA Glenn Research Center. For this contribution, the author is very appreciative. Also, the work of Michael

Penson, an undergraduate student at UAHuntsville is greatly appreciated. Without his assistance in sample preparation, profilometry, and other necessary tasks, these results would not have been obtained. James Mulroy, another undergraduate student at UAHuntsville, also helped with the mass measurements, and this is acknowledged. Finally, the data entry performed by Sarah Evans was greatly appreciated.

References

1. A.S. Khanna, *Introduction to High Temperature Oxidation and Corrosion*, ASM International, Materials Park, OH, 2002
2. E. Andrieu et al., Intergranular Crack Tip Oxidation Mechanism in a Nickel-Based Superalloy, *Mater. Sci. Eng. A*, 1992, **154**, p 21–28
3. J.L. Evans, "Environment Assisted Crack Growth in Ni-Base Superalloys at Elevated Temperature," Ph.D. Dissertation, University of Arkansas, 2008
4. J.C. Arnault et al., Roughness Fractal Approach of Oxidised Surfaces by AFM and Diffuse X-Ray Reflectometry Measurements, *Appl. Surf. Sci.*, 2001, **171**, p 189–196
5. S. Uran et al., Effect of Surface Roughness on Oxidation: Changes in Scale Thickness, Composition, Residual Stress, *Oxidat. Met.*, 2000, **54**(1/2), p 73–85
6. A.M. Huntz, Roughness and Oxidation: Application to NiO Growth on Ni at 800°C, *Mater. Sci. Eng. A*, 2000, **290**, p 190–197
7. Zhang et al., Effect of Surface Roughness on the Development of Protective Al_2O_3 on Fe–10Al (at.%) Alloys Containing 0–10 at.% Cr, *Appl. Surf. Sci.*, 2006, **253**, p 881–888